Electromagnetically Induced Transparency with Amplification in Superconducting Circuits

Jaewoo Joo,[1] Jérôme Bourassa,[2] Alexandre Blais,[2] and Barry C. Sanders[1]
[1]*Institute for Quantum Information Science, University of Calgary, Alberta T2N 1N4, Canada*
[2]*Département de Physique, Université de Sherbrooke, Sherbrooke, Québec J1K 2R1, Canada*
(Received 11 April 2010; published 9 August 2010)

We show that controlling relative phases of electromagnetic fields driving an atom with a Δ-configuration energy-level structure enables optical susceptibility to be engineered in novel ways. In particular, relative-phase control can yield electromagnetically induced transparency but with the benefit that the transparency window is sandwiched between an absorption and an amplification band rather than between two absorption bands in typical electromagnetically induced transparency. We show that this new phenomenon is achievable for a microwave field interacting with a fluxonium superconducting circuit.

DOI: 10.1103/PhysRevLett.105.073601 PACS numbers: 42.50.Gy, 42.50.Md, 74.50.+r

An electromagnetically driven three-level atom with a Δ electronic-energy structure, denoted Δ3LA and depicted in Fig. 1, yields an optical susceptibility with interesting and important properties. The Δ3LA has been investigated theoretically [1] and experimentally [2,3]. For example, electromagnetically induced transparency (EIT) [4] arises by pumping the $|2\rangle \leftrightarrow |3\rangle$ transition so that the $|1\rangle \leftrightarrow |3\rangle$ transition can controllably be made either absorptive or transparent to a resonant driving field, thereby enabling slowing of light pulses. Alternatively, lasing without inversion (LWI) [5], corresponding to amplification despite the absence of population inversion, can be achieved by also pumping the $|1\rangle \leftrightarrow |2\rangle$, thereby providing a second excitation pathway. Here we show that the Δ3LA susceptibility for the $|1\rangle \leftrightarrow |3\rangle$ can be tailored by controlling the relative phases of the fields pumping the $|1\rangle \leftrightarrow |3\rangle$ and $|1\rangle \leftrightarrow |2\rangle$ transitions, thereby yielding a combination of EIT and LWI, which we call "electromagnetically induced transparency with amplification" (EITA). Our theory of phase-controlled doubly driven Δ3LA predicts asymmetric EIT peaks, commensurate with experimental observations of an anomalous asymmetry of EIT peaks for Rb Δ3LAs [3], and we show that this novel system can be realized with an artificial Δ3LA based on superconducting circuits.

Superconducting circuit quantum electrodynamics (CQED) has replicated many quantum optical phenomena, including strong dipole coupling [6], Autler-Townes splitting [7], coherent population trapping [8], the Mollow triplet [9], and EIT [10], by coupling a nonlinear electronic circuit to a microwave field passing through a nearby transmission line. The nonlinear circuit is engineered to produce just a few relevant energy levels, thereby behaving as an "artificial atom." One important subtlety in translating atomic experiments to superconducting CQED is that, in the optical case, the electromagnetic field is in three dimensions and undergoes scattering, absorption, and dispersion, whereas, in the superconducting CQED case, the passing microwave field is transmitted or reflected with complex parameters characterizing the strengths and phases of the reflected and transmitted fields. Another subtlety is that superconducting CQED typically employs just one artificial atom, whereas many atoms are usually coupled to the field in the optical case. Last, EIT for superconducting circuits with energy levels in a Λ configuration has been studied theoretically previously [11,12].

The Δ3LA depicted in Fig. 1 has three energy levels $|i\rangle$ with frequency differences ω_{ij} and decay rates γ_{ij} between levels $|i\rangle$ and $|j\rangle$ for $i, j \in \{1, 2, 3\}$. The $|i\rangle \leftrightarrow |j\rangle$ transition with electric-dipole vector $\boldsymbol{d}_{ij}$ is driven by a coherent electromagnetic field with electric field $\boldsymbol{E}_{ij}$ and detuning δ_{ij} from resonance with that transition. The corresponding (complex) Rabi frequency is $\Omega_{ij} = \boldsymbol{d}_{ij} \cdot \boldsymbol{E}_{ij}$ ($\hbar \equiv 1$). As will be seen below, in some circumstances, selection rules do not apply to superconducting circuits, so all dipole transitions can be driven by applying a trichromatic microwave field tuned near each of the ω_{ij} [13].

For $\hat{\sigma}_{ij} := |i\rangle\langle j|$, the system Hamiltonian is

$$\hat{H} = \sum_{i=1}^{3} \omega_i \hat{\sigma}_{ii} - \frac{1}{2}\sum_{i>j} (\Omega_{ij} e^{-i(\omega_{ij}+\delta_{ij})t} \hat{\sigma}_{ij} + \text{H.c.}), \quad (1)$$

with H.c. denoting the Hermitian conjugate. In the rotating frame with $\delta_{12} = \delta_{13} - \delta_{23}$, Eq. (1) becomes

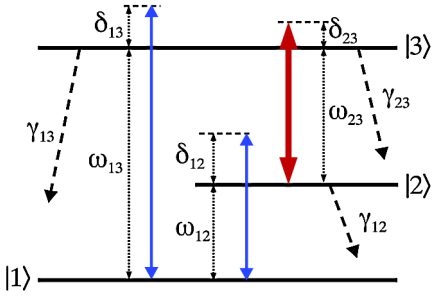

FIG. 1 (color online). Δ3LA system with driving fields indicated by solid arrows (blue and red), decays by dashed lines, and frequency differences between levels by dotted lines.

$$\hat{H}_{\rm int} = -\sum_{i=2}^{3} \delta_{1i}\hat{\sigma}_{ii} - \frac{1}{2}\sum_{i>j}(\Omega_{ij}\hat{\sigma}_{ij} + \text{H.c.}). \quad (2)$$

Energy relaxation and dephasing caused by coupling to uncontrolled degrees of freedom are described by a Lindblad-type master equation

$$\dot{\rho} = -i[\hat{H}_{\rm int}, \rho] + \mathcal{D}\Big[\sum_{i<j}\sqrt{\gamma_{ij}}\sigma_{ij}\Big]\rho + \mathcal{D}\Big[\sum_{i=2}^{3}\sqrt{\gamma_{\phi i}}\sigma_{ii}\Big]\rho =: \mathcal{L}\rho \quad (3)$$

for $\mathcal{D}[c]\bullet := c\bullet\hat{c}^{\dagger} - \{\hat{c}^{\dagger}c, \bullet\}/2$. Here $\gamma_{\phi i}$ is a pure dephasing rate for level $|i\rangle$, which should be negligible for flux Δ3LAs at the flux degeneracy point [14] and for fluxonium Δ3LAs in a wider range of flux around this degeneracy point [15].

For EIT, a strong pump field $\Omega_{23} \gg \Omega_{13} > 0$ causes Autler-Townes splitting of level $|3\rangle$ yielding two absorption peaks at $\delta_{13}/\gamma_{13} = \pm|\Omega_{23}|/2\Gamma_3$ for $\Gamma_3 = (\gamma_{13} + \gamma_{23} + \gamma_{\phi 3})/2$ with a transparency window centered at $\delta_{13} = 0$ and full width at half maximum FWHM $= \gamma_{12} + \gamma_{\phi 2} + |\Omega_{23}|^2/2\Gamma_3$ [16]. Optical dispersion and absorption are quantified, respectively, by the real and imaginary parts of the first-order susceptibility $\chi^{(1)} \propto |d_{13}|^2\rho^s_{31}/\Omega_{13}$, with $\rho^s_{ij} = \langle i|\rho^s|j\rangle$ the steady-state solution of the master equation [12]. Hence, dispersion and absorption are proportional to $\mathrm{Re}[\rho^s_{31}]$ and $\mathrm{Im}[\rho^s_{31}]$, shown in Figs. 2(a) and 2(b) for EITA, EIT ($\Omega_{12} = 0$), and LWI ($\Omega_{13} = 0$). As expected, these dispersion and absorption curves are related by the Kramers-Kronig relation.

The EIT absorption curve exhibits a transparency window between two Autler-Townes peaks, and the linear dispersion curve in Fig. 2(b) indicates that the group velocity is constant and lower in this window. The LWI absorption curve shows the characteristic transparency at resonance with absorption in the red-detuned (left) region and amplification (or negative absorption) in the blue-detuned (right) region. EITA exhibits the transparency window characteristic of EIT but with the LWI feature that the window is bounded by an absorption and an amplification peak rather than by two Autler-Townes absorption peaks. Figure 2(c) confirms that population inversion $\rho^s_{11} - \rho^s_{33}$ is always positive for EIT, LWI, and EITA, so amplification is not due to population inversion.

In fact, EITA is not a simple combination of EIT and LWI as coherence between levels adds to the richness of the phenomenon. As depicted in Fig. 3, due to interlevel coherence, controlling the relative phase of (at least) one field with respect to the other two affects whether amplification is in the red- or blue-detuned region or even whether there is amplification at all. This control becomes evident by taking $\rho^s_{23} \approx 0$ [17]:

$$\rho^s_{31} = -e^{-i\phi_{13}}[2i\Omega_{13}(\rho^s_{11} - \rho^s_{33})(i\delta_{13} - \gamma_{12}/2) + \Omega_{23}\Omega_{12}e^{-i(\phi_{12}+\phi_{23}-\phi_{13})}(\rho^s_{11} - \rho^s_{22})]/F, \quad (4)$$

where $F = 4(i\delta_{13} - \Gamma_3)(i\delta_{13} - \gamma_{12}/2) + \Omega^2_{23}$ and clearly depicts contributions from the standard EIT (first term) and LWI (second term) effects. Interference between the two effects is controlled by the relative phase $\Phi := \phi_{12} + \phi_{23} - \phi_{13}$, where we observe that the absorption curve of Fig. 2(a) is recovered for $\Phi = 0$. EITA is replaced by ordinary absorption for $\Phi = \pi/2$ with $\gamma_{12} \ll \gamma_{13}$, and the mirror image of the $\Phi = 0$ absorption curve occurs for $\Phi = \pi$. For $\Phi = 3\pi/2$, the absorption curve corresponds to an EIT profile but with the transparency window replaced by an amplification window and with a linear dispersion profile, so group velocity is constant and slower for this window.

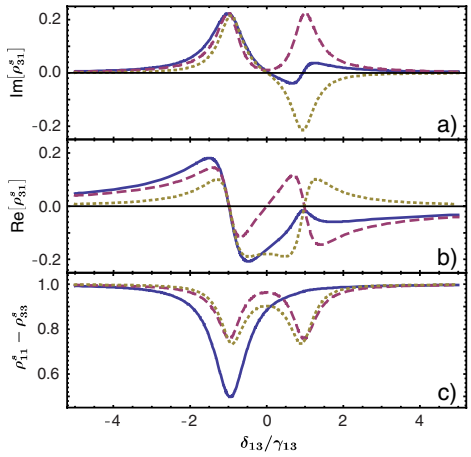

FIG. 2 (color online). (a) Absorption, (b) dispersion, and (c) population inversion vs detuning δ_{13}/γ_{13} for EIT (red dashed lines), LWI (yellow dotted lines), and EITA (blue solid lines) for $10\gamma_{12} = \gamma_{13}$, $\gamma_{23} = \gamma_{12}$, $\delta_{23} = 0$, $5\Omega_{13} = 5\Omega_{12} = \gamma_{13}$, and $\Omega_{23} = \gamma_{13}$.

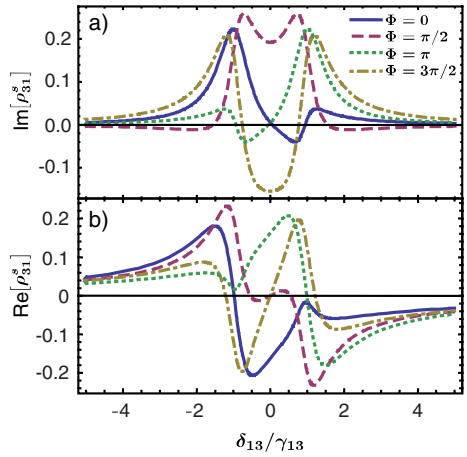

FIG. 3 (color online). (a) Absorption and (b) dispersion vs detuning δ_{13}/γ_{13} as obtained from the steady state of Eq. (3) for Φ equal to 0 (solid blue line), $\pi/2$ (dashed red line), π (dotted green line), and $3\pi/2$ (dash-dotted yellow line). Parameters are the same as in Fig. 2.

Our theory of a Δ3LA is applicable to a recent EIT experiment with Rb atomic gas [3], which exhibited both transmission enhancement and asymmetry between the red- and blue-detuned transmission peaks. Their theory [3] explains transmission enhancement but not the observed peak asymmetry. As the lower two levels of their Rb 3LA are driven by a microwave field, they have a Δ3LA; thus, our theory predicts peak asymmetry. A quantitative analysis is required to see how much of the asymmetry is due to Δ structure effects rather than other reasons. We note that, while our theory also predicts negative absorption (amplification), inhomogeneous broadening and absorption in the gas cell could obscure the amplification signature. An advantage of our proposal to study EITA with superconducting artificial atoms coupled to one-dimensional transmission lines is that EITA can be investigated in a controlled way without some of the complications that arise for gases.

Flux [18] and fluxonium [15] 3LAs closely approximate Δ3LAs away from flux degeneracy [13] and, hence, are natural candidates for realizing EITA. Figure 4(a) shows the energy levels structure of the fluxonium 3LA and Fig. 4(b) the corresponding transition matrix elements $|t_{ij}| = |d_{ij}|/g$, with g being the electric-dipole coupling frequency, both as a function of the externally applied flux Φ_{ext}. Away from $\Phi_{\text{ext}}/\Phi_0 = 0$ and 0.5, all three matrix elements have comparable values such that the fluxonium can be used as a Δ system. Flux 3LAs have similar magnetic flux transition matrix elements [13] but are more sensitive to flux noise and tend to have the state $|3\rangle$ high in energy. Under these considerations, the fluxonium appears to be a promising candidate for the observation of the effect studied here.

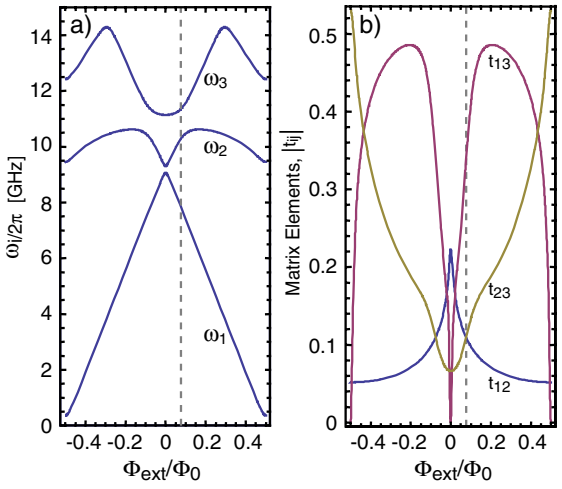

FIG. 4 (color online). (a) Transition frequencies $\omega_i/2\pi$ and (b) coupling matrix elements $|t_{ij}|$ for charge coupling in the fluxonium Δ3LA between states $|i\rangle$ and $|j\rangle$ as a function of the external flux Φ_{ext}/Φ_0, with Φ_0 being the flux quantum. Parameters are from Ref. [15]. We suggest biasing the artificial 3LA at $\Phi_{\text{ext}}/\Phi_0 = 0.08$, indicated by a dashed vertical line, where $t_{12} = t_{23}$, optimal for observation of EITA.

The susceptibility, and hence EITA, can be probed by connecting either 3LA to a transmission line supporting traveling modes [9]. The absorption and dispersion profiles can be measured in both transmission and reflection, and a possible setup for homodyne measurement of the reflected signal is illustrated in Fig. 5. To determine how much information about ρ_{31} resides in the reflected signal, we use input-output theory [19]. In the Markov approximation and focusing on the signals centered about the probe (a), pump (b), and control (c) frequencies, the transmission-line free Hamiltonian is

$$\hat{H}_{\text{TL}} = \sum_{\hat{o}\in\{\hat{a},\hat{b},\hat{c}\}} \int_0^\infty d\omega \hat{o}^\dagger(\omega)\hat{o}(\omega), \tag{5}$$

with the microwave field annihilation operators $\hat{o}(\omega)$ satisfying $[\hat{o}(\omega), \hat{o}'^\dagger(\omega')] = \delta_{\hat{o},\hat{o}'}\delta(\omega - \omega')$.

Treating the transmission-line mode as three commuting quasimonochromatic modes is valid if separation between the transitions frequencies greatly exceeds the linewidths. In this approximation, the Δ3LA-transmission line interaction Hamiltonian is

$$\hat{H}_{\text{int}} = i\int_{-\infty}^{\infty} d\omega\Big[\sqrt{\frac{\gamma_{13}}{2\pi}}\hat{a}^\dagger(\omega)\hat{\sigma}_{13} + \sqrt{\frac{\gamma_{23}}{2\pi}}\hat{b}^\dagger(\omega)\hat{\sigma}_{23} + \sqrt{\frac{\gamma_{12}}{2\pi}}\hat{c}^\dagger(\omega)\hat{\sigma}_{12} - \text{H.c.}\Big]. \tag{6}$$

By using input-output theory, the output field operator centered at the probe frequency is then $\hat{a}_{\text{out}}(t) = \hat{a}_{\text{in}}(t) + \sqrt{\gamma_{13}}\hat{\sigma}_{13}(t)$, with $\hat{a}_{\text{in}}(t)$ the annihilation operator for the input field centered at the probe frequency. With the homodyne setup illustrated in Fig. 5 effectively measuring $\langle\hat{a}_{\text{out}}(t)\rangle = \langle\hat{a}_{\text{in}}(t)\rangle + \sqrt{\gamma_{13}}\rho_{31}(t) \equiv r\langle\hat{a}_{\text{in}}(t)\rangle$, access to the dispersion and absorption profiles is straightforward

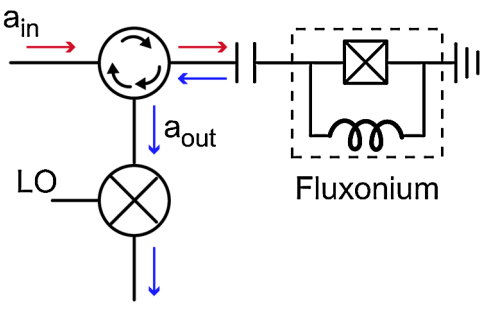

FIG. 5 (color online). A fluxonium 3LA, made from the parallel combination of a Josephson junction and a large inductance, is capacitively coupled to the end of a semi-infinite transmission line and measured in reflection. A circulator is used to separate the input and output fields. The output field is amplified (not shown) and mixed with a local oscillator (LO) to realize a homodyne measurement.

through measurement of the imaginary and real parts of the reflection coefficient r, respectively,

We propose to bias the fluxonium at $\Phi_{\text{ext}}/\Phi_0 = 0.08$, indicated by a dashed vertical line in Fig. 4, where $t_{12} = t_{23}$ as this choice is optimal for observation of EITA. Contrary to the case of resonators [20], coupling to the transmission-line traveling modes exposes the Δ3LA to environmental vacuum fluctuations of the voltage at the Δ3LA transition frequencies, thereby enhancing spontaneous decay. As an estimate for the relaxation time in this case, we use Astafiev *et al.*'s results, where a flux qubit was coupled to a transmission line with $\gamma_{12}/2\pi = 11$ MHz at zero flux [9]. Assuming white noise, the decay rates at $\Phi_{\text{ext}}/\Phi_0 = 0.08$ can be estimated by using the matrix elements of Fig. 4, yielding $\gamma_{13}/2\pi = 25$ MHz, $\gamma_{12}/2\pi = 2.6$ MHz, and $\gamma_{23}/2\pi = 2.6$ MHz. Figures 2 and 3 have been obtained by using these values, showing that EITA with superconducting Δ3LA should be possible with current experimental parameters.

Another approach to probing EITA with superconducting circuits is by quantum state tomography, where the density matrix is fully reconstructed, demonstrating the noninversion of the population in the amplification window. This can be done, for example, by coupling the Δ3LA to a resonator rather than a transmission line [21], and strong coupling of a flux Δ3LA to a resonator has been studied [22–24]. An advantage of this approach is that the resonator shields the Δ3LA from noise away from the resonator frequency, thereby decreasing significantly the decay rates.

In summary, we have developed the theory of EITA and shown how it can be implemented in superconducting circuit QED. The EITA effect is obtained by engineering the susceptibility of the Δ3LA by controlling the amplitude and relative phases of the microwaves driving fields. We suggest a homodyne measurement scheme for the direct observation of the susceptibility, and thereby the EITA absorption and dispersion profiles of the probe field, with a fluxonium artificial atom fabricated at the end of a one-dimensional transmission line. EITA is exciting as EIT and LWI are found to occur and combine in novel ways within a single system, and superconducting CQED realizations enable its controlled study. Finally, an array of superconducting Δ3LA could represent an essential building block for quantum communication and quantum computation as the EITA effect and coherent control of the susceptibility enables slowing, storage, and amplification of microwave fields on demand.

This project is supported by FQRNT, NSERC, CIFAR, *iCORE*, and QuantumWorks. We thank S. Filipp for discussions about the phase control of multiple microwave drives. A. B. is partially supported by the Alfred P. Sloan Foundation.

[1] D. Kosachiov *et al.*, Opt. Commun. **85**, 209 (1991); D. Kosachiov and E. A. Korsunsky, Eur. Phys. J. D **11**, 457 (2000).
[2] Y. Zhao *et al.*, Phys. Rev. Lett. **79**, 641 (1997); E. A. Wilson *et al.*, Phys. Rev. A **72**, 063813 (2005).
[3] H. Li *et al.*, Phys. Rev. A **80**, 023820 (2009).
[4] M. Fleischhauer *et al.*, Rev. Mod. Phys. **77**, 633 (2005).
[5] S. E. Harris, Phys. Rev. Lett. **62**, 1033 (1989); M. O. Scully, S. Y. Zhu, and A. Gavrielides, Phys. Rev. Lett. **62**, 2813 (1989).
[6] A. Wallraff *et al.*, Nature (London) **431**, 162 (2004).
[7] M. Baur *et al.*, Phys. Rev. Lett. **102**, 243602 (2009); M. A. Sillanpaa *et al.*, Phys. Rev. Lett. **103**, 193601 (2009).
[8] W. Kelly *et al.*, Phys. Rev. Lett. **104**, 163601 (2010).
[9] O. Astafiev *et al.*, Science **327**, 840 (2010).
[10] A. A. Abdumalikov, Jr. *et al.*, arXiv:1004.2306v1.
[11] Z. Dutton *et al.*, Phys. Rev. B **73**, 104516 (2006); K. V. R. M. Murali *et al.*, Phys. Rev. Lett. **93**, 087003 (2004).
[12] H. Ian *et al.*, Phys. Rev. A **81**, 063823 (2010).
[13] Y.-x. Liu *et al.*, Phys. Rev. Lett. **95**, 087001 (2005).
[14] P. Bertet *et al.*, Phys. Rev. Lett. **95**, 257002 (2005).
[15] V. E. Manucharyan *et al.*, Science **326**, 113 (2009).
[16] E. Figueroa *et al.*, Opt. Lett. **31**, 2625 (2006).
[17] For the parameters of Fig. 2, we find $\max[|\rho_{23}^s|] \approx 0.15$; hence, the approximation $\rho_{23}^s \approx 0$ suffices to obtain the features qualitatively but not quantitatively.
[18] J. E. Mooij *et al.*, Science **285**, 1036 (1999).
[19] C. W. Gardiner and M. J. Collett, Phys. Rev. A **31**, 3761 (1985).
[20] A. Blais *et al.*, Phys. Rev. A **69**, 062320 (2004); Z. Dutton *et al.*, Phys. Rev. B **73**, 104516 (2006); K. V. R. M. Murali *et al.*, Phys. Rev. Lett. **93**, 087003 (2004).
[21] S. Filipp *et al.*, Phys. Rev. Lett. **102**, 200402 (2009).
[22] J. Bourassa *et al.*, Phys. Rev. A **80**, 032109 (2009).
[23] A. A. Abdumalikov, Jr. *et al.*, Phys. Rev. B **78**, 180502 (2008).
[24] T. Niemczyk *et al.*, arXiv:1003.2376 [Nature Phys. (to be published)].